

Patterns of New Physics in $b \rightarrow s\ell^+\ell^-$ transitions in the light of recent data

Bernat Capdevila^a, Andreas Crivellin^b, Sébastien Descotes-Genon^c, Joaquim Matias^a and Javier Virto^d

^a*Universitat Autònoma de Barcelona, 08193 Bellaterra, Barcelona, Institut de Física d'Altes Energies (IFAE),
The Barcelona Institute of Science and Technology, Campus UAB, 08193 Bellaterra (Barcelona), Spain*

^b*Paul Scherrer Institut, CH-5232 Villigen PSI, Switzerland*

^c*Laboratoire de Physique Théorique, UMR 8627,*

CNRS, Univ. Paris-Sud, Université Paris-Saclay, 91405 Orsay Cedex, France

^d*Albert Einstein Center for Fundamental Physics, Institute for Theoretical Physics,
University of Bern, CH-3012 Bern, Switzerland*

(Dated: April 19, 2017)

The $b \rightarrow s\ell^+\ell^-$ processes observed by the LHCb collaboration at 1 and 3 fb⁻¹ have exhibited a coherent set of deviations from the Standard Model (SM) predictions, i.e., anomalies, most remarkably in the angular analysis of the $B \rightarrow K^*\mu^+\mu^-$ decay and in the Lepton Flavour Universality (LFU) violating ratios R_K and (very recently) R_{K^*} . All these anomalies are analysed consistently by fitting the Wilson coefficients of effective operators which encode the short-distance contributions to $b \rightarrow s\ell^+\ell^-$ transitions, pointing towards specific patterns of New Physics (NP). We include recent data presented by LHCb, CMS, ATLAS and Belle in our framework, finding several hypotheses with NP in one and two Wilson coefficients preferred at the 5 σ level compared to the SM. One of the most prominent patterns consist of large contributions to the coefficients $C_{9\mu}$ ($C_{10\mu}$) involving a left-handed quark current and a vector (axial) muon current while the effect in electrons is small, confirming the indications for LFU violation. We also perform an analysis allowing for New Physics in six Wilson coefficients (SM-like and chirally flipped), obtaining a pull for the SM at the level of 5 σ . Dedicated fits restricted to LFU-violating observables are also presented. We find that LFU violation is favoured with respect to LFU at 3.3 σ level in the case of NP contributions to C_{9e} and $C_{9\mu}$. Finally, we consider the implications of these results for specific models of NP and we discuss possible correlations to the LFU-violating ratios R_D and R_{D^*} .

1. INTRODUCTION

The discovery of the Higgs boson marked the completion of the Standard Model (SM) of particle physics. Now, the main focus has shifted to the identification of physics beyond the SM. While the LHC has not observed new heavy particles directly, indirect searches through flavour observables have been evolving from a precision study of the SM towards a search tool for New Physics (NP). Over the last few years, many observables related to the flavour-changing neutral-current transitions $b \rightarrow s\ell^+\ell^-$ have exhibited deviations from SM expectations. Due to their suppression within the SM, these transitions are well known to have a high sensitivity to potential NP contributions.

In 2013, using the 1fb⁻¹ dataset, the LHCb experiment measured the basis of optimised observables [1] for $B \rightarrow K^*\mu^+\mu^-$ [2], observing the so-called P'_5 anomaly [3], i.e., a sizeable 3.7 σ discrepancy between the measurement and the SM prediction in one bin for the angular observable P'_5 [4]. In 2015, using the 3 fb⁻¹ dataset, LHCb confirmed this discrepancy with a 3 σ deviation in each of two adjacent bins at large K^* recoil [5]. LHCb also observed a systematic deficit with respect to SM predictions for the branching ratios of several decays, such as $B_s \rightarrow \phi\mu^+\mu^-$ [6, 7]. In 2016, the Belle experiment presented an independent analysis of P'_5 [8, 9] confirming the LHCb measurements in a very different experimental setting.

A conceptually new element arose when a discrepancy in the ratio $R_K = \mathcal{B}_{B \rightarrow K\mu^+\mu^-} / \mathcal{B}_{B \rightarrow Ke^+e^-}$ was also observed by LHCb [10], hinting at the violation of lepton flavour universality (LFU) and suggesting that deviations from the SM are predominantly present in $b \rightarrow s\mu^+\mu^-$ transitions but not in $b \rightarrow se^+e^-$ ones. Recently Belle has measured for the first time [9] the additional LFU violating (LFUV) observables $Q_{4,5} = P_{4,5}^{\mu\mu} - P_{4,5}^{ee}$, proposed in Ref. [11]. Even if not yet statistically significant, the result points also towards LFUV in Q_5 , consistently with R_K . A list of the most prominent anomalies is presented in Table I.

This situation is *exceptional* in the sense that the observed deviations form coherent patterns and can be explained consistently within the model-independent approach of the effective Hamiltonian governing the $b \rightarrow s\ell\ell$ transitions. Indeed, some of these patterns of NP are significantly preferred compared to the SM, solving the deviations observed in many measurements from different experiments. First in Ref. [3] (using only $B \rightarrow K^*\mu\mu$) and later on in Ref. [12] (with all LHCb data available at that time) it was shown that a very economical mechanism, namely a negative contribution of the order of -25% to the short-distance coefficient of the effective operator $\mathcal{O}_9^\mu = e^2/(16\pi^2) (\bar{s}\gamma_\mu P_L b) (\bar{\mu}\gamma^\mu \mu)$ is sufficient to alleviate all above-mentioned tensions, whereas the data allowed for NP contributions to other operators. It was found that this solution is favoured over the SM with a large significance (between 4 and 5 σ). This picture was

Largest pulls	$\langle P'_5 \rangle_{[4,6]}$	$\langle P'_5 \rangle_{[6,8]}$	$R_K^{[1,6]}$	$R_{K^*}^{[0.045, 1.1]}$	$R_{K^*}^{[1.1, 6]}$	$\mathcal{B}_{B_s \rightarrow \phi \mu^+ \mu^-}^{[2,5]}$	$\mathcal{B}_{B_s \rightarrow \phi \mu^+ \mu^-}^{[5,8]}$
Experiment	-0.30 ± 0.16	-0.51 ± 0.12	$0.745^{+0.097}_{-0.082}$	$0.66^{+0.113}_{-0.074}$	$0.685^{+0.122}_{-0.083}$	0.77 ± 0.14	0.96 ± 0.15
SM prediction	-0.82 ± 0.08	-0.94 ± 0.08	1.00 ± 0.01	0.92 ± 0.02	1.00 ± 0.01	1.55 ± 0.33	1.88 ± 0.39
Pull (σ)	-2.9	-2.9	+2.6	+2.3	+2.6	+2.2	+2.2
Prediction for $\mathcal{C}_{9\mu}^{\text{NP}} = -1.1$	-0.50 ± 0.11	-0.73 ± 0.12	0.79 ± 0.01	0.90 ± 0.05	0.87 ± 0.08	1.30 ± 0.26	1.51 ± 0.30
Pull (σ)	-1.0	-1.3	+0.4	+1.9	+1.2	+1.8	+1.6

TABLE I: Main anomalies currently observed in $b \rightarrow s \ell \ell$ transitions, with the current measurements, our predictions for the SM and the NP scenario $\mathcal{C}_{9\mu}^{\text{NP}} = -1.1$, and the corresponding pulls. In addition, a deficit compared to the SM predictions has been observed at low and large recoils for $\mathcal{B}(B^{(0,+)} \rightarrow K^{(0,+)} \mu \mu)$ [13] and $\mathcal{B}(B^0 \rightarrow K^{*0} \mu \mu)$ [14], as well as at low recoil (above 15 GeV²) for $\mathcal{B}(B^+ \rightarrow K^{*+} \mu^+ \mu^-)$ [13] and $\mathcal{B}(B_s \rightarrow \phi \mu^+ \mu^-)$ [7].

confirmed by other global analyses [15–17] using different observables, hadronic inputs and theory approaches for their computations. Controversies on hadronic uncertainties (power corrections to form factors [18, 19], charm-loop contributions [20, 21]) have been addressed and resolved in Refs. [22–25].

Recently, the experimental picture has changed significantly. The ATLAS and CMS collaborations have presented new preliminary results for optimized observables: ATLAS measured the whole set as well as F_L at large K^* recoil [26], whereas CMS presented results for P_1 and P'_5 at low and large recoils [27]. The results show a good (but not perfect) overall agreement with the LHCb results, and a global model-independent analysis [28] has confirmed the earlier picture in Refs. [3, 12, 15–17] on many issues: favoured hypotheses for NP contributions to Wilson Coefficients, consistency of deviation patterns in the various channels and types of observables, robustness with respect to the theoretical assumptions on hadronic corrections, and absence of q^2 - or helicity-dependences for $\mathcal{C}_{9,\mu}^{\text{NP}}$ that would signal uncontrolled long-distance contributions in $B \rightarrow K^* \mu^+ \mu^-$.

On the other hand, the LHCb collaboration has recently updated the differential branching ratio for $B \rightarrow K^* \mu^+ \mu^-$ [14], and it has presented striking new results concerning the LFUV ratio $R_{K^*} = \mathcal{B}(B \rightarrow K^* \mu^+ \mu^-) / \mathcal{B}(B \rightarrow K^* e^+ e^-)$ at large K^* recoil [29], exhibiting significant deviations from SM expectations. Ratios like R_K and R_{K^*} are particularly interesting due to their lack of sensitivity to hadronic uncertainties, their precise prediction within the SM and their potential to discriminate among NP models [30, 31]. The significant deviation of R_{K^*} from SM expectations confirm in particular that hadronic uncertainties in the theoretical predictions are not sufficient to explain all the anomalies observed in $b \rightarrow s \ell^+ \ell^-$ transitions, and that alternative explanations must be searched for.

In this note, we discuss how these remarkable new results affect the global model-independent analysis of NP in $b \rightarrow s \ell^+ \ell^-$ decays, we determine patterns of NP contributions favoured by the whole set of experimental data, and we study their implications for NP models. The structure of this note is the following: In Sec. 2, we briefly recall the framework used for our global analysis, focus-

ing on the changes compared to our previous work [12]. In Sec. 3, we present the results for different hypotheses of NP contributions to the short-distance Wilson coefficients. In Sec. 4, we consider the consequences for well-motivated models of NP, before drawing our conclusions. Further detail on the computation of R_{K^*} , the connection with $R_{D^{(*)}}$ and some implications for future LFUV observables are discussed in the appendices.

2. FRAMEWORK

We perform a global fit to all available $b \rightarrow s \gamma$ and $b \rightarrow s \ell^+ \ell^-$ data along the lines of Ref. [12], to determine the best-fit points and the confidence-level intervals for the Wilson coefficients $\mathcal{C}_{9,10}^{(\prime)} e, \mu$ (see [3] for definitions). We include all the observables considered in the reference fit of Ref. [12] (see Secs. 2 and 3, and App. A of this reference). More specifically, for the angular observables in $B \rightarrow K^* \mu^+ \mu^-$, $B \rightarrow K^* e^+ e^-$ and $B_s \rightarrow \phi \mu^+ \mu^-$, we use the optimised observables $P_i^{(\prime)}$ obtained from LHCb's likelihood fit [5]. Concerning the q^2 binning we use the finest bins at large recoil (below the J/ψ) but the widest bins in the low-recoil region to ensure quark-hadron duality. For the $b \rightarrow s \gamma$ radiative observables, we add to our previous set of observables the branching ratios of the radiative decays $B^0 \rightarrow K^{*0} \gamma$, $B^+ \rightarrow K^{*+} \gamma$, $B_s \rightarrow \phi \gamma$ [32].

We add to the fit all the new measurements made available since Ref. [12]:

- The $B^0 \rightarrow K^{*0} \mu^+ \mu^-$ differential branching fraction measured by LHCb [14] based on the full run 1 dataset, superseding the results in Ref. [33]. A recent update of Ref. [14] led to a reduction of the branching ratio by about 20% in magnitude.
- The new Belle measurements [9] for the isospin-averaged but lepton-flavour dependent $B \rightarrow K^* \ell^+ \ell^-$ observables $P'_{4,5} e$ and $P'_{4,5} \mu$. The isospin average is given by the following expression [34]

$$P_i^{\prime \ell} = \sigma_+ P_i^{\prime \ell}(B^+) + (1 - \sigma_+) P_i^{\prime \ell}(\bar{B}^0). \quad (1)$$

Since σ_+ describing the relative weight of each isospin component in the average is not public, we treat it as a nuisance parameter $\sigma_+ = 0.5 \pm 0.5$. This will not

1D Hyp.	All					LFUV				
	Best fit	1 σ	2 σ	Pull _{SM}	p-value	Best fit	1 σ	2 σ	Pull _{SM}	p-value
$\mathcal{C}_{9\mu}^{\text{NP}}$	-1.10	[-1.27, -0.92]	[-1.43, -0.74]	5.7	72	-1.76	[-2.36, -1.23]	[-3.04, -0.76]	3.9	69
$\mathcal{C}_{9\mu}^{\text{NP}} = -\mathcal{C}_{10\mu}^{\text{NP}}$	-0.61	[-0.73, -0.48]	[-0.87, -0.36]	5.2	61	-0.66	[-0.84, -0.48]	[-1.04, -0.32]	4.1	78
$\mathcal{C}_{9\mu}^{\text{NP}} = -\mathcal{C}'_{9\mu}$	-1.01	[-1.18, -0.84]	[-1.33, -0.65]	5.4	66	-1.64	[-2.12, -1.05]	[-2.52, -0.49]	3.2	31
$\mathcal{C}_{9\mu}^{\text{NP}} = -3\mathcal{C}_{9e}^{\text{NP}}$	-1.06	[-1.23, -0.89]	[-1.39, -0.71]	5.8	74	-1.35	[-1.82, -0.95]	[-2.38, -0.59]	4.0	71

2D Hyp.	All			LFUV		
	Best fit	Pull _{SM}	p-value	Best fit	Pull _{SM}	p-value
$(\mathcal{C}_{9\mu}^{\text{NP}}, \mathcal{C}_{10\mu}^{\text{NP}})$	(-1.17, 0.15)	5.5	74	(-1.13, 0.40)	3.7	75
$(\mathcal{C}_{9\mu}^{\text{NP}}, \mathcal{C}'_7)$	(-1.05, 0.02)	5.5	73	(-1.75, -0.04)	3.6	66
$(\mathcal{C}_{9\mu}^{\text{NP}}, \mathcal{C}_{9'\mu})$	(-1.09, 0.45)	5.6	75	(-2.11, 0.83)	3.7	73
$(\mathcal{C}_{9\mu}^{\text{NP}}, \mathcal{C}_{10'\mu})$	(-1.10, -0.19)	5.6	76	(-2.43, -0.54)	3.9	85
$(\mathcal{C}_{9\mu}^{\text{NP}}, \mathcal{C}_{9e}^{\text{NP}})$	(-0.97, 0.50)	5.4	72	(-1.09, 0.66)	3.5	65
Hyp. 1	(-1.08, 0.33)	5.6	77	(-1.74, 0.53)	3.8	77
Hyp. 2	(-1.00, 0.15)	4.9	61	(-1.89, 0.27)	3.1	39
Hyp. 3	(-0.65, -0.13)	4.9	61	(0.58, 2.53)	3.7	73
Hyp. 4	(-0.65, 0.21)	4.8	59	(-0.68, 0.28)	3.7	72

TABLE II: Most prominent patterns of New Physics in $b \rightarrow s\mu\mu$ with high significances. The last four rows corresponds to hypothesis 1: ($\mathcal{C}_{9\mu}^{\text{NP}} = -\mathcal{C}_{9'\mu}, \mathcal{C}_{10\mu}^{\text{NP}} = \mathcal{C}_{10'\mu}$), 2: ($\mathcal{C}_{9\mu}^{\text{NP}} = -\mathcal{C}_{9'\mu}, \mathcal{C}_{10\mu}^{\text{NP}} = -\mathcal{C}_{10'\mu}$), 3: ($\mathcal{C}_{9\mu}^{\text{NP}} = -\mathcal{C}_{10\mu}^{\text{NP}}, \mathcal{C}_{9'\mu} = \mathcal{C}_{10'\mu}$) and 4: ($\mathcal{C}_{9\mu}^{\text{NP}} = -\mathcal{C}_{10\mu}^{\text{NP}}, \mathcal{C}_{9'\mu} = -\mathcal{C}_{10'\mu}$). The “All” columns include all available data from LHCb, Belle, ATLAS and CMS, whereas the “LFUV” columns are restricted to R_K , R_{K^*} and $Q_{4,5}$ (see text for more detail). The p -values are quoted in % and Pull_{SM} in units of standard deviation.

have a significant effect in our results, since the isospin breaking in the SM is small (but accounted for in our analysis), and we do not consider NP contributions to four-quark operators.

► The new ATLAS measurements [26] on the angular observables P_1 , $P'_{4,5,6,8}$ in $B^0 \rightarrow K^{*0}\mu^+\mu^-$ as well as F_L in the large recoil region.

► The new CMS measurements [27] on the angular observables P_1 and P'_5 in $B^0 \rightarrow K^{*0}\mu^+\mu^-$, both at large and low recoils (we consider only the [16,19] bin at low recoil). We take F_L and A_{FB} from an earlier analysis [35]. We also include the data from an earlier analysis at 7 TeV [36]. A very welcome check of the stability of the CMS results would consist in performing a simultaneous extraction of F_L , P_1 and P'_5 , using the same folding distribution as ATLAS, LHCb and Belle.

► The new measurements of the lepton-flavour non-universality ratio R_{K^*} in two large-recoil bins by the LHCb collaboration [29]. The likelihood of these measurements is asymmetric, and dominated by statistical uncertainties. We thus take the two measurements as uncorrelated, and for each of the two bins, we take a symmetric Gaussian error that is the larger of the two asymmetric uncertainties (while keeping the central value unchanged). This approach makes us underestimate the impact of these measurements on our fit, but it is conservative until the likelihood is known in detail.

Following Ref. [12], we take into account the corre-

lations whenever available, and assume that the measurements are uncorrelated otherwise. In order to avoid including measurements with too large correlations, we include the LHCb measurements of the ratios R_{K^*} and R_K , as well as the differential branching ratios $\mathcal{B}(B^0 \rightarrow K^{*0}\mu\mu)$ and $\mathcal{B}(B^+ \rightarrow K^+\mu\mu)$, but we discard $\mathcal{B}(B^0 \rightarrow K^{*0}ee)^{[0.0009,1]}$ and $\mathcal{B}(B^+ \rightarrow K^+ee)^{[1,6]}$.

Regarding the theory computation of all observables, we follow Refs. [12, 22], which take into account the theoretical updates for the branching ratios of $B \rightarrow X_s\gamma$, $B \rightarrow X_s\mu\mu$ and $B_s \rightarrow \mu\mu$ in Refs. [37–39]. For $B \rightarrow K^*$ form factors at large recoil we use the calculation in Ref. [40], which has more conservative uncertainties than the ones in Ref. [41], obtained with a different method. For $B_s \rightarrow \phi$ the corresponding calculation is not available, and therefore we use Ref. [41]. This leads to smaller hadronic uncertainties quoted for $B_s \rightarrow \phi\ell\ell$ and R_ϕ , but we stress that this is only due to the choice of input.

We follow the same statistical method as in Ref. [12]: We perform a frequentist analysis with all known theory and experimental correlations taken into account through the covariance matrix when building the χ^2 function, which is minimised to find best-fit points, pulls, p -values and confidence-level intervals. Depending on the dimensionality of the hypothesis, the minimisation is performed either using a simple scan or the Markov-Chain Monte Carlo Metropolis-Hastings algorithm.

	$\mathcal{C}_7^{\text{NP}}$	$\mathcal{C}_{9\mu}^{\text{NP}}$	$\mathcal{C}_{10\mu}^{\text{NP}}$	$\mathcal{C}_{7'}$	$\mathcal{C}_{9'\mu}$	$\mathcal{C}_{10'\mu}$
Best fit	+0.017	-1.12	+0.33	+0.03	+0.59	+0.07
1 σ	[-0.01, +0.05]	[-1.34, -0.85]	[+0.09, +0.59]	[+0.00, +0.06]	[+0.01, +1.12]	[-0.23, +0.37]
2 σ	[-0.03, +0.07]	[-1.51, -0.61]	[-0.10, +0.80]	[-0.02, +0.08]	[-0.50, +1.56]	[-0.50, +0.64]

TABLE III: 1 and 2 σ confidence intervals for the NP contributions to Wilson coefficients in the six-dimensional hypothesis allowing for NP in $b \rightarrow s\mu\mu$ operators dominant in the SM and their chirally-flipped counterparts. The SM pull is 4.9 σ (fit “All” including CMS data at both 7 and 8 TeV) or 5.0 σ (fit “All” with only the latest CMS data at 8 TeV included).

3. RESULTS

We discuss now several hypotheses for NP contributions in various Wilson coefficients. We consider real contributions, and consistently we have not included CP -violating observables in our fits. In Table II we give the fit results for several one- or two-dimensional hypothesis for NP contributions to $b \rightarrow s\mu\mu$ operators, with two different datasets: either we include all available data from muon and electron channels presented in the previous section (column “All”, 175 measurements), or we include only LFUV observables, i.e., R_K and R_{K^*} from LHCb and Q_i ($i = 4, 5$) from Belle, where $Q_i = P'_{i\mu} - P'_{ie}$ was discussed in Ref. [11] (column “LFUV”, 17 measurements). In both cases, we include also the $b \rightarrow s\gamma$ observables, as well as $\mathcal{B}(B \rightarrow X_s\mu\mu)$ and $\mathcal{B}(B_s \rightarrow \mu\mu)$. The SM point yields a χ^2 corresponding to a p -value of 14.6% for the fit “All” and 4.4% for the fit “LFUV”.

We start by discussing NP hypotheses for the fit “All”. The measurement of R_{K^*} increases further the significance of already prominent hypotheses in previous studies, namely, the first three hypotheses ($\mathcal{C}_{9\mu}^{\text{NP}}$, $\mathcal{C}_{9\mu}^{\text{NP}} = -\mathcal{C}_{10\mu}^{\text{NP}}$ and $\mathcal{C}_{9\mu}^{\text{NP}} = -\mathcal{C}_{9'\mu}$) already identified in Refs. [3, 12]. The SM pull exceeds 5 σ in each case: the hypotheses can hardly be distinguished on this criterion, and as discussed in Ref. [11], the Q_i observables will be very powerful tools to lift this quasi-degeneracy.

Besides providing one- and two-dimensional hypotheses with SM pulls above 5 σ , we discuss four illustrative examples (useful for model building) of constrained hypotheses among a larger set of Wilson coefficients. Hypothesis 1 has the highest SM pull in agreement with our previous global analysis [12]. Changing relative signs between the constrained coefficients: taking $\mathcal{C}_{10\mu}^{\text{NP}} = -\mathcal{C}_{10'\mu}$ (i.e., Hypothesis 2) reduces the significance from 5.6 σ to 4.9 σ , similarly to hypotheses taking $\mathcal{C}_{9\mu}^{\text{NP}} = -\mathcal{C}_{10\mu}^{\text{NP}}$ (irrespectively of the relative sign taken to constrain $\mathcal{C}_{9'\mu} = \pm\mathcal{C}_{10'\mu}$). From a model-independent point of view, Hypothesis 1 is particularly interesting to yield a low value for R_{K^*} (especially if a contribution $\mathcal{C}_7^{\text{NP}} > 0$ is allowed). Let us add that a scenario with only $\mathcal{C}_{9\mu}^{\text{NP}} = -\mathcal{C}_{9'\mu}$ would predict $R_K = 1$ and $R_{K^*} < 1$ [12, 30, 31, 50]. One could however obtain $R_K < 1$ by adding a positive contribution to $\mathcal{C}_{10\mu}$ and/or $\mathcal{C}_{10'\mu}$ (see Tab. 9 in Ref. [12]).

Up to now, we have discussed scenarios where NP contributions occur only in $b \rightarrow s\mu\mu$ transitions. It is also interesting to consider scenarios with NP in both muon and electron channels, in particular $(\mathcal{C}_{9\mu}^{\text{NP}}, \mathcal{C}_{9e}^{\text{NP}})$, with a

SM pull of 5.4 σ , and a p -value of 72%. While $\mathcal{C}_{9\mu}^{\text{NP}} \sim -1$ is preferred over SM with a significance in the 5 σ region, \mathcal{C}_{9e} is compatible with SM already at 1 σ , in agreement with the LFUV data included in the fit. One can assess more precisely the need for LFUV in the framework where NP is allowed in both $(\mathcal{C}_{9e}^{\text{NP}}, \mathcal{C}_{9\mu}^{\text{NP}})$ through the pull of the hypothesis $(\mathcal{C}_{9e}^{\text{NP}} = \mathcal{C}_{9\mu}^{\text{NP}})$ which reaches 3.3 σ . Considering the results for the $(\mathcal{C}_{9e}^{\text{NP}}, \mathcal{C}_{9\mu}^{\text{NP}})$ hypothesis, one can notice that a very good fit is also obtained for the one-dimensional hypothesis $\mathcal{C}_{9\mu}^{\text{NP}} = -3\mathcal{C}_{9e}^{\text{NP}}$ favoured in some models discussed in the next section.

In the upper row of Fig. 1, we show the corresponding constraints for the fit “All” under the three hypotheses $(\mathcal{C}_{9\mu}^{\text{NP}}, \mathcal{C}_{10\mu}^{\text{NP}})$, $(\mathcal{C}_{9\mu}^{\text{NP}}, \mathcal{C}_{9\mu'})$ and $(\mathcal{C}_{9\mu}^{\text{NP}}, \mathcal{C}_{9e}^{\text{NP}})$, as well as the 3 σ regions according to the results from individual experiments (for each region, we add the constraints from $b \rightarrow s\gamma$ observables, $\mathcal{B}(B \rightarrow X_s\mu\mu)$ and the world average for $\mathcal{B}(B_s \rightarrow \mu\mu)$ [32]). As expected, the LHCb results drive most of the effect, with a clear exclusion of the origin, i.e., the SM point.

We can now move to the fit “LFUV” in the lower row of Fig. 1, where we consider the same hypotheses favoured by global analyses. It is interesting to notice that this restricted subset of observables excludes the SM point with a high significance, and it favours regions similar to the fit “All” dominated by different $b \rightarrow s\mu\mu$ -related observables ($B \rightarrow K^*\mu\mu$ optimised angular observables as well as low- and large-recoil branching ratios for $B \rightarrow K\mu\mu$, $B \rightarrow K^*\mu\mu$ and $B_s \rightarrow \phi\mu\mu$). This is also shown in Tab II where the scenarios with the highest pulls are confirmed with significances between 3 and 4 σ , but get harder to distinguish on the basis of their significance. Scenarios like $\mathcal{C}_{9\mu}^{\text{NP}} = -\mathcal{C}_{9'\mu}$ that would fail to explain R_K are not disfavoured due to their good compatibility with R_{K^*} data.

Finally, we have performed a six-dimensional fit allowing for NP contributions in $\mathcal{C}_{7(\prime),9(\prime)\mu,10(\prime)\mu}$. The SM pull has shifted from 3.6 σ in Ref. [12] to the level of 5 σ with the inclusion of the recent data: it reaches 4.9 σ if one considers the fit “All” described above, and 5.0 σ if the CMS data considered in this fit is restricted to the latest 8 TeV dataset [27]. The 1 and 2 σ CL intervals (identical in both cases) are given in Tab. III, with the pattern:

$$\mathcal{C}_7^{\text{NP}} \gtrsim 0, \mathcal{C}_{9\mu}^{\text{NP}} < 0, \mathcal{C}_{10\mu}^{\text{NP}} > 0, \mathcal{C}_7' \gtrsim 0, \mathcal{C}_{9'\mu} > 0, \mathcal{C}_{10'\mu} \gtrsim 0 \quad (2)$$

where $\mathcal{C}_{9\mu}$ is compatible with the SM beyond 3 σ , $\mathcal{C}_{10\mu}$, $\mathcal{C}_{7'}$ and $\mathcal{C}_{9'}$ at 2 σ and all the other coefficients at 1 σ .

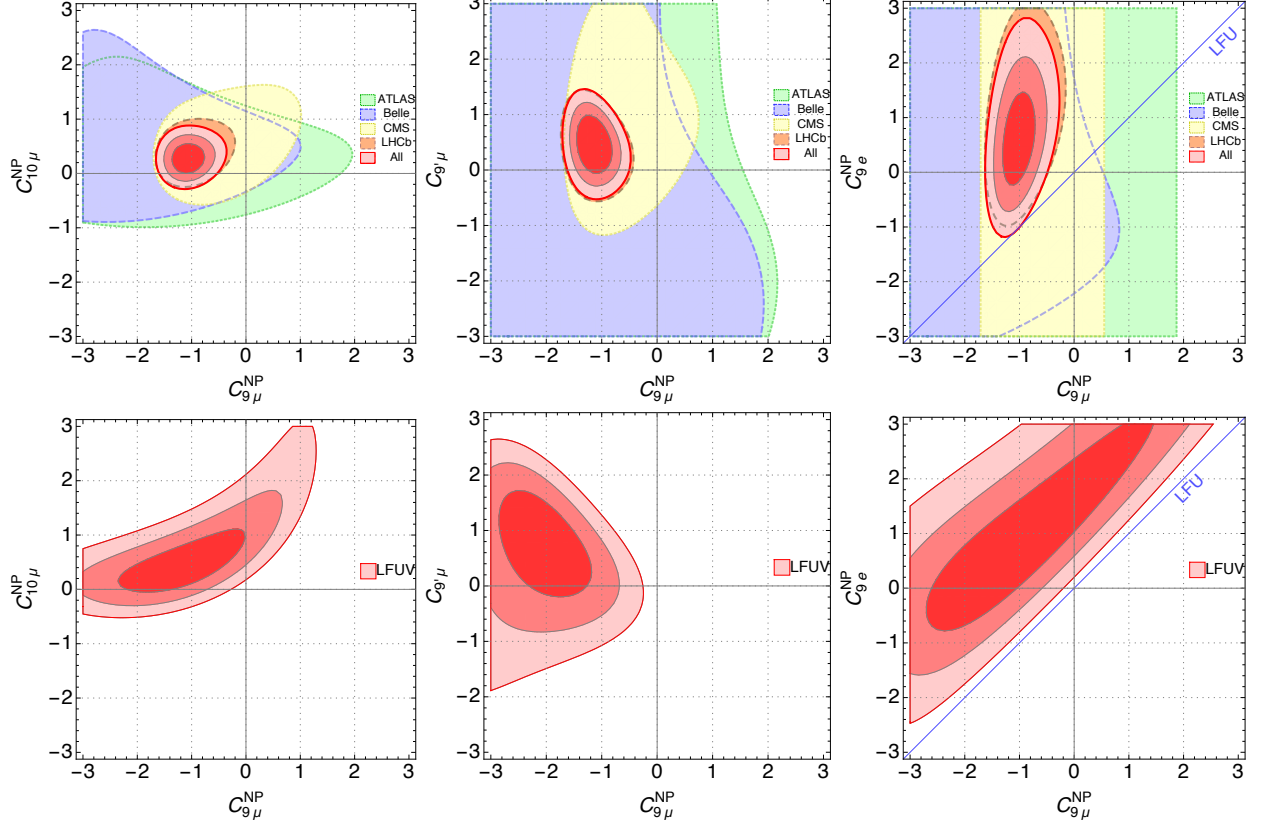


FIG. 1: From left to right: Allowed regions in the $(C_{9\mu}^{NP}, C_{10\mu}^{NP})$, $(C_{9\mu}^{NP}, C_{9'\mu}^{NP})$ and $(C_{9\mu}^{NP}, C_{9e}^{NP})$ planes for the corresponding two-dimensional hypotheses, using all available data (upper row, fit “All”) and only LFUV observables (lower row, fit “LFUV”). We also show the 3σ regions for the data subsets corresponding to specific experiments. Constraints from $b \rightarrow s\gamma$ observables, $\mathcal{B}(B \rightarrow X_s \mu \mu)$ and $\mathcal{B}(B_s \rightarrow \mu \mu)$ are included in each case (see text).

4. IMPLICATIONS FOR MODELS

Our updated model-independent fit to available $b \rightarrow s\ell\ell$ and $b \rightarrow s\gamma$ data strongly favours LFUV scenarios with NP affecting mainly $b \rightarrow s\mu\mu$ transitions, with a preference for the three hypotheses $C_{9\mu}^{NP}$, $C_{9\mu}^{NP} = -C_{10\mu}^{NP}$ and $C_{9\mu}^{NP} = -C_{9'\mu}^{NP}$. This has important implications for some popular ultraviolet-complete models which we briefly discuss.

► **LFUV**: Given that leptoquarks (LQs) should possess very small couplings to electrons in order to avoid dangerous effects in $\mu \rightarrow e\gamma$, they naturally violate LFU. While Z' models can easily accommodate LFUV data, LFU variants like the ones in Refs. [42, 43] are now disfavoured. The same is true if one aims at explaining P'_5 via NP in four-quark operators leading to a NP (q^2 -dependent) contribution from charm loops [44]. Models with right-handed currents such as Refs. [45, 50] are also strongly disfavoured, even though they can account for R_K , since they would result in $R_{K^*} > 1$.

► **$C_{9\mu}^{NP}$** : Z' models with fundamental (gauge) couplings to leptons preferably yield $C_{9\mu}^{NP}$ -like solutions in order

to avoid gauge anomalies. In this context, $L_\mu - L_\tau$ models [46–49] are popular since they do not generate effects in electron channels. The new fit including R_{K^*} is also very favourable to models predicting $C_{9\mu}^{NP} = -3C_{9e}^{NP}$ [51]. Interestingly, such a symmetry pattern is in good agreement with the structure of the PMNS matrix [52]. Concerning LQs, a $C_{9\mu}^{NP}$ -like solution can only be generated by adding two scalar (an $SU(2)_L$ triplet and an $SU(2)_L$ doublet with $Y = 7/6$) or two vector representations (an $SU(2)_L$ singlet with $Y = 2/3$ and an $SU(2)_L$ doublet with $Y = 5/6$).

► **$C_{9\mu}^{NP} = -C_{10\mu}^{NP}$** : This pattern can be achieved in Z' models with loop-induced couplings [53] or in Z' models with heavy vector-like fermions [54] which possess also LFUV. Concerning LQs, here a single representation (the scalar $SU(2)_L$ triplet or the vector $SU(2)_L$ singlet with $Y = 2/3$) can generate a $C_{9\mu} = -C_{10\mu}$ like solution [55–60] and this pattern can also be obtained in models with loop contributions from three heavy new scalars and fermions [61–63].

► **$C_{9\mu}^{NP} = -C_{9'\mu}^{NP}$** : This pattern could be generated in Z' models with vector-like fermions. For the $L_\mu - L_\tau$

model [46] this would be naturally the case if vector-like fermions and the generalized Yukawa couplings respect a left-right symmetry. One could also obtain this pattern by adding a third Higgs doublet to the model of Ref. [47] with opposite $U(1)$ charge. Generating $\mathcal{C}_{9\mu}^{\text{NP}} = -\mathcal{C}_{9'\mu}^{\text{NP}}$ in LQ models requires one to add four scalar representations or three vector ones.

Concerning the constrained hypotheses in the lower part of Tab II, only two of them (2 and 4) can be explained within a Z' model, while hypothesis 1 and 3 violate the relationship $\mathcal{C}_{9\mu}^{\text{NP}} \times \mathcal{C}_{10'\mu} = \mathcal{C}_{10\mu}^{\text{NP}} \times \mathcal{C}_{9'\mu}$ [12] that minimal Z' models should obey. One would have to turn to other models (like LQs with a sufficient number of representations) to explain the hypothesis with the highest pull (Hyp. 1). A possible correlation with $R_{D^{(*)}}$ of one of the scenarios is discussed in App. B.

5. CONCLUSIONS AND OUTLOOK

Over the last years, a very interesting pattern of deviations has emerged in the Flavour-Changing Neutral Current $b \rightarrow s\ell\ell$ transitions. After the initial P'_5 anomaly identified in $B \rightarrow K^*\mu\mu$ by the LHCb experiment, several deviations have been observed in various branching ratios, and finally, several observables comparing electron and muon modes have been measured at LHCb (R_K) and Belle ($Q_{4,5}$) hinting at a violation of lepton flavour universality. These deviations have been analysed by several groups through the model-independent approach of the effective Hamiltonian, favouring NP contributions to $b \rightarrow s\mu\mu$ transitions, dominantly in the semileptonic operator $\mathcal{O}_{9\mu}$, whereas $b \rightarrow see$ transitions are little affected. Several NP hypotheses, corresponding to contributions to specific Wilson coefficients, improve in a consistent way all the deviations observed.

This picture has been updated recently in a remarkable manner. The ATLAS and CMS experiments have performed angular analyses of the $B^0 \rightarrow K^{*0}\mu\mu$ decay. But more strikingly, LHCb has presented new results for the LFUV ratio R_{K^*} deviating from SM expectations in two bins at low recoil and confirming their observation of a violation of LFU in $b \rightarrow s\ell\ell$ modes. This remarkable measurement calls for a reassessment of our previous analysis, which we have presented here.

As before, a large NP contribution to $\mathcal{C}_{9\mu}$ is favoured by the data, whereas there is no need for a similar NP contribution to the electron mode. We have identified one- and two-dimensional hypotheses with real NP contributions to Wilson coefficients that improve significantly the agreement between data and predictions compared to the SM, reaching significances between 5σ and 6σ , and we have given the corresponding p -values and confidence intervals for the NP contributions. We have also performed fits restricted to LFUV observables, showing that even this very restrictive set of observables favours several NP hypotheses compared to the SM in a very significant way, yielding confidence regions that are qualitatively similar

to the results of the global fits. A six-dimensional fit to $\mathcal{C}_{7(\prime)}, \mathcal{C}_{9(\prime)\mu}, \mathcal{C}_{10(\prime)\mu}$ confirms the need for a large contribution to $\mathcal{C}_{9\mu}$ and hints at contributions in $\mathcal{C}_{9'\mu}$ and/or $\mathcal{C}_{10\mu}$, with a SM pull of 5.0σ . We have discussed the consequences of the favoured hypotheses for models such as leptoquarks and Z' boson, in connection with the deviations also observed in $R_{D^{(*)}}$.

The strong hints of NP observed here call for further cross checks. Additional data on $b \rightarrow s\ell\ell$ as well as new observables [11, 64] are naturally important to make further progress and sharpen the constraints from global analyses. In particular, more accurate measurements of $B_s \rightarrow \mu\mu$ observables [65, 66] will help in constraining the value of $\mathcal{C}_{10\mu}$, which is slightly away from zero according to our global analysis. On the theoretical side, if hadronic uncertainties seem now under control and unexpectedly large effects (power corrections to form factors, charm-loop contributions) are disfavoured by the significant LFUV observed, it would be very useful to have more determinations of the form factors involved, both at low and large meson recoils, in order to improve the accuracy of theoretical predictions.

Depending on the models, the strong hints of LFUV NP observed here can be related to other sectors. In the case of left-handed NP contributions explaining LFUV in both $b \rightarrow s\ell\ell$ and $b \rightarrow c\ell\nu$, $b \rightarrow s\tau\tau$ should be enhanced by up to three orders of magnitude (within the reach of LHCb and Belle II) [75]. On the other hand, leptoquark models explaining the same deviations yield large branching ratios (of order 10^{-5}) for $b \rightarrow s\tau\mu$, and they provide predictions for $\mathcal{B}(K \rightarrow \pi\mu\mu)/\mathcal{B}(K \rightarrow \pi ee)$ to be measured at NA62 or KOTO [67]. In addition, one should investigate lepton-flavour violating processes such as lepton-flavour-violating decays for the H boson and for charged leptons, $\tau \rightarrow \mu\nu\nu$, etc.

We have been able to identify different NP hypotheses reaching significances above 5σ , but it remains to determine which of the different scenarios will prevail in order to provide definite directions for model building. The remarkable measurements obtained by the LHCb collaboration for R_{K^*} should be a strong incentive to additional tests of the violation of lepton flavour universality. This should be done through more statistics, different decay modes (such as R_K with a finer binning, or R_ϕ for $B_s \rightarrow \phi\ell\ell$), different observables (such as the optimised observables Q_i discussed with other LFUV observables in Ref. [11]), and different experimental settings (such as Belle II). These measurements should prove highly instrumental in exploiting the full potential of $b \rightarrow s\ell\ell$ decays to search for New Physics and ultimately uncover its detailed pattern.

Acknowledgments

This work received financial support from the grant FPA2014-61478-EXP [JM, SDG, BC, JV] and from Centro de Excelencia Severo Ochoa SEV-2012-0234 [BC];

from the EU Horizon 2020 program from the grants No 690575, No 674896 and No. 692194 [SDG]. The work of A.C. is supported by an Ambizione Grant of the Swiss National Science Foundation (PZ00P2_154834). J.V. is funded by the Swiss National Science Foundation.

Appendix A: A closer look at R_{K^*}

In this appendix we comment on a few issues concerning the recent measurement of R_{K^*} . First, hadronic uncertainties cancel to a large extent in the SM in this type of LFUV observables. However, even in the SM, in the first bin (below 1 GeV²), where contributions proportional to the difference of lepton masses are $1/q^2$ -enhanced due to the presence of the photon pole, one should expect larger errors than above 1 GeV² [11, 23]. In addition, in the presence of NP, the theoretical uncertainty could be magnified in these observables defined as ratios of branching ratios, as the cancellation of hadronic uncertainties is not as efficient as in the SM, so that the error depends strongly on the LCSR form factors used to compute these observables. This enhancement of the uncertainty is less important in the optimised LFUV observables Q_i . An exception to this enhancement occurs under the hypothesis $\mathcal{C}_{9\mu}^{\text{NP}} = -\mathcal{C}_{10\mu}^{\text{NP}}$: above 1 GeV², because the contribution of right-handed amplitudes to R_{K^*} cancel mostly, reducing the theoretical uncertainty substantially.

Large-recoil expressions for the transversity amplitudes can be used as a testing ground (see Ref. [11] and [23] for exact predictions) to provide approximate expressions for R_{K^*} in the first two bins in terms of Wilson coefficients (only $\mathcal{C}_{9,10,9',10'}^\ell$ and $\mathcal{C}_{7,7'}$). Let us stress that the following approximate expressions are given for illustrative purposes, and that complete expressions have been used for all the numerical evaluations in this article.

Under this approximation one can explore different mechanisms/scenarios to explain data. In the first bin one finds:

$$R_{K^*}^{[0.045,1.1]} \simeq \left(12.8 + g_{(1)}^\mu + g_{(2)}^\mu\right) / \left(13.4 + g_{(1)}^e + g_{(2)}^e\right)$$

where $g_{(i)}^\ell$ stands for the linear ($i = 1$) and quadratic ($i = 2$) term for $\ell = e, \mu$ and are given by:

$$g_{(1)}^\ell = -1.1 [\mathcal{C}_{10\ell}^{\text{NP}} - \mathcal{C}_{9\ell}^{\text{NP}}/2 + \mathcal{C}_{9'\ell} - \mathcal{C}_{10'\ell}] - 61.9 \mathcal{C}_7^{\text{NP}} - 1.7 \mathcal{C}_7' \quad (\text{A1})$$

and

$$g_{(2)}^\ell = -0.7 \mathcal{C}_7^{\text{NP}} \mathcal{C}_7' + 123.1 [(\mathcal{C}_7^{\text{NP}})^2 + (\mathcal{C}_{7'}^{\text{NP}})^2] + 2.2 [\mathcal{C}_7^{\text{NP}} \mathcal{C}_{9\ell}^{\text{NP}} + \mathcal{C}_{7'}^{\text{NP}} \mathcal{C}_{9'\ell}] + 0.1 [(\mathcal{C}_{9\ell}^{\text{NP}})^2 + (\mathcal{C}_{10\ell}^{\text{NP}})^2 + (\mathcal{C}_{9'\ell})^2 + (\mathcal{C}_{10'\ell})^2] - 0.4 \left[\mathcal{C}_7^{\text{NP}} \mathcal{C}_{9'\ell} + \mathcal{C}_7' \mathcal{C}_{9\ell}^{\text{NP}} + \frac{1}{2} (\mathcal{C}_{9\ell}^{\text{NP}} \mathcal{C}_{9'\ell} + \mathcal{C}_{10\ell}^{\text{NP}} \mathcal{C}_{10'\ell}) \right] \quad (\text{A2})$$

showing that a negative (positive) contribution to $\mathcal{C}_{9\mu}^{\text{NP}}$ and $\mathcal{C}_{10'\mu}$ ($\mathcal{C}_{10\mu}^{\text{NP}}$ and $\mathcal{C}_{9'\mu}$) enhances the deviation from SM. The (universal) radiative coefficients \mathcal{C}_7 and $\mathcal{C}_{7'}$ play also a (subleading) role in mixed terms combining them with the semileptonic NP coefficients in this bin.

In the second bin, the expression gets simplified due to the very limited impact on R_{K^*} of the radiative coefficients \mathcal{C}_7 and $\mathcal{C}_{7'}$ (not shown here):

$$R_{K^*}^{[1.1,6]} \simeq \left(29.2 + \tilde{g}_{(1)}^\mu + \tilde{g}_{(2)}^\mu\right) / \left(29.3 + \tilde{g}_{(1)}^e + \tilde{g}_{(2)}^e\right) \quad (\text{A3})$$

with

$$\tilde{g}_{(1)}^\ell = -8.1 \mathcal{C}_{10\ell}^{\text{NP}} + 5.3 \mathcal{C}_{10'\ell} + 5.6 \mathcal{C}_{9\ell}^{\text{NP}} - 5.0 \mathcal{C}_{9'\ell} \quad (\text{A4})$$

and

$$\tilde{g}_{(2)}^\ell = +0.9 [(\mathcal{C}_{10\ell}^{\text{NP}})^2 + (\mathcal{C}_{10'\ell})^2 + (\mathcal{C}_{9\ell}^{\text{NP}})^2 + (\mathcal{C}_{9'\mu})^2] - 1.2 [\mathcal{C}_{9\ell}^{\text{NP}} \mathcal{C}_{9'\ell} + \mathcal{C}_{10\ell}^{\text{NP}} \mathcal{C}_{10'\ell}] \quad (\text{A5})$$

In the presence of NP, the same mechanisms as in the first bin operate here, but with a stronger impact.

A last comment is in order concerning the relatively low value of R_{K^*} in the first bin. It is difficult to accommodate a very low value of R_{K^*} in this first bin through NP contributions to semileptonic $\mathcal{C}_{9\mu}, \mathcal{C}_{10\mu}$ coefficients (in agreement with the fit), since the branching ratio gets dominated by the photon pole from the LFU operator \mathcal{O}_7 . A low value can be obtained if a positive contribution $\mathcal{C}_7^{\text{NP}} = \mathcal{O}(0.1)$ is added together with a small positive (negative) contribution to $\mathcal{C}_{9'\mu}$ ($\mathcal{C}_{10'\mu}$), but such a large contribution is however not favoured by $b \rightarrow s\gamma$ observables. Moreover, the second bin will be even lower than the first one. It seems thus likely that the very low value of the first bin for R_{K^*} is partly due to a downward statistical fluctuation.

Appendix B: Correlations with $R_{D^{(*)}}$

It is interesting to correlate the violation of lepton flavour universality observed in $b \rightarrow s\ell\ell$ with the measurements of R_D and R_{D^*} that also point towards LFUV in B decays with a significance of 3.9σ [32].

A solution of the $R_{D^{(*)}}$ anomaly can naturally be achieved with a NP contribution to the SM operator $\bar{c}\gamma^\mu P_L b \bar{\tau}\gamma_\mu P_L \nu$ as it complies with the B_c lifetime [68] and q^2 distributions [69–71]. Assuming $SU(2)$ invariance, the effect in $R_{D^{(*)}}$ is correlated to $b \rightarrow s\ell^+\ell^-$ and/or to $b \rightarrow s\nu\bar{\nu}$, following the pattern $\mathcal{C}_{9\mu} = -\mathcal{C}_{10\mu}$. Following model-independent arguments, $b \rightarrow s\tau^+\tau^-$ must then be significantly enhanced. Indeed, since $b \rightarrow c\ell\nu$ processes are mediated already at tree level in the SM, a rather large NP contribution is required and in principle large contributions to $b \rightarrow s\nu\bar{\nu}$ processes appear, due to $SU(2)$ invariance. These bounds from $B \rightarrow K^{(*)}\nu\bar{\nu}$ can be avoided if the coupling structure is mainly aligned to the third generation but this disagrees with direct LHC

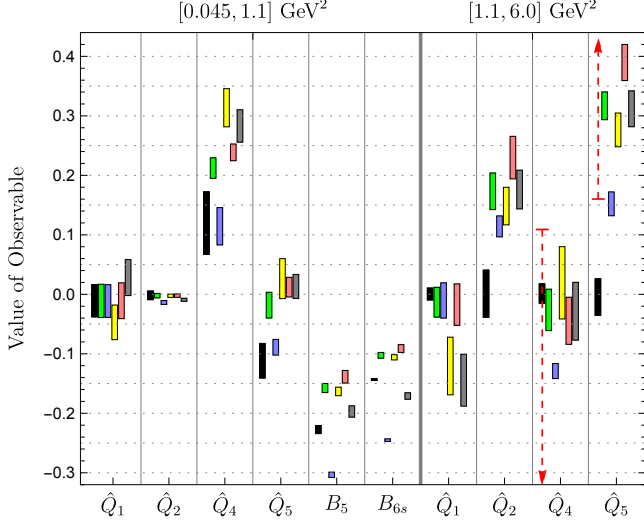


FIG. 2: Predictions and experimental measurements for the \hat{Q}_i and B_5 , B_{6s} observables in specific bins. In each case, from left to right, the predictions are given for the SM (filled black box) and for the Scenarios 1 to 5 (in this order) defined in App. C. The dashed red interval corresponds to the experimental measurement, when available.

searches [72] and electroweak precision observables [73]. However, there is no effect in $b \rightarrow s\nu\bar{\nu}$ processes in the case of a contribution $\mathcal{C}_1^{\text{NP}} = -\mathcal{C}_3^{\text{NP}}$ to gauge-invariant operators [74], which can be achieved with the vector LQ $SU(2)$ singlet [58, 59] or with a combination of two scalar LQs [75]. In both cases large effects in $b \rightarrow s\tau^+\tau^-$ (of the order of 10^{-3} for $B_s \rightarrow \tau^+\tau^-$) are predicted [75].

Assuming that the coupling to the second generation is sizeable in order to avoid the bounds from direct LHC searches and electroweak precision observables one finds

$$\mathcal{C}_{9(10)\tau} \approx \mathcal{C}_{9(10)}^{\text{SM}} - (+)2\frac{\pi}{\alpha}\frac{V_{cb}}{V_{ts}}\left(\sqrt{\frac{R_{D^{(*)}}}{R_{D^{(*)}}^{\text{SM}}}} - 1\right). \quad (\text{B1})$$

Furthermore, in LQ models one expects sizeable branching ratios for $b \rightarrow s\tau\mu$ processes, reaching 10^{-5} [75].

Appendix C: Future opportunities for LFUV

The best NP scenarios obtained from the global fits have a similar goodness of fit and describe the anomalies with an equivalent success. New measurements will determine eventually which scenario gets singled out. In this respect, a few of the optimised observables measuring LFUV proposed in Ref. [11] are particularly promising, with pioneering measurements from the Belle experiment for $Q_{4,5}$ [9].

In order to illustrate the future potential for establishing which one (if any) of the various NP scenarios is preferred, we consider not only $R_{K,K^*,\phi}$ but also the observables $\hat{Q}_{1,2,4,5}$ and $B_{5,6s}$ in the same q^2 bins as

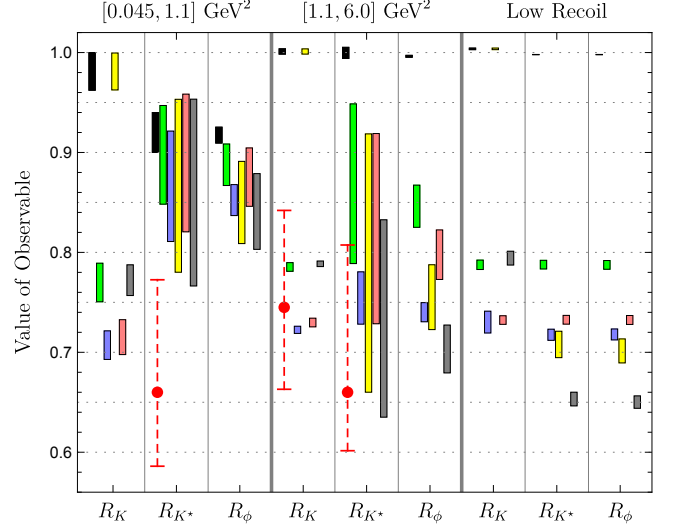


FIG. 3: Predictions and experimental measurements for R_K , R_{K^*} and R_ϕ with the same conventions as Fig. 2. In the central box, the predictions for R_K are given for the bin $[1,6]$ GeV^2 , whereas R_{K^*} and R_ϕ are given in $[1.1,6]$ GeV^2 . The low-recoil bin corresponds to $[15,22]$ GeV^2 , $[15,19]$ GeV^2 or $[15,18.8]$ GeV^2 for R_K , R_{K^*} and R_ϕ respectively. The smaller uncertainties in R_ϕ (compared to R_{K^*}) is due to the choice of form factors in each case, see Sec. 2.

the R_{K^*} LHCb measurements: $[0.045, 1.1]$, $[1.1, 6.0]$ and $[15, 19]$ GeV^2 , and calculate the predictions within the SM as well as within five “good” scenarios from Section 3:

- Scenario 1: $\mathcal{C}_{9\mu}^{\text{NP}} = -1.1$,
- Scenario 2: $\mathcal{C}_{9\mu}^{\text{NP}} = -\mathcal{C}_{10\mu}^{\text{NP}} = -0.61$,
- Scenario 3: $\mathcal{C}_{9\mu}^{\text{NP}} = -\mathcal{C}'_{9\mu} = -1.01$,
- Scenario 4: $\mathcal{C}_{9\mu}^{\text{NP}} = -3\mathcal{C}_{9e}^{\text{NP}} = -1.06$,
- Scenario 5: The best fit point in the six-dimensional fit (Table III).

The results are summarised in Figs. 2 and 3, where we show only the most interesting cases. We find that:

- As it is well known, R_K cannot distinguish between Scenario 3 and the SM, but it is optimal to identify NP in the case of Scenarios 1, 2 and 4. However, it cannot distinguish well among them. This is true in all the three bins considered here. R_{K^*} has large uncertainties at large recoil, but it has good sensitivity to Scenario 2 in the bin $[1.1, 6]$ (although difficult to distinguish from the other NP scenarios). In the same bin R_ϕ is slightly better. The low-recoil bin of R_{K^*} and R_ϕ is particularly promising to decouple Scenarios 1 and 5 from each other and the SM, but only if experimental uncertainties are small.

- $\langle \hat{Q}_2 \rangle^{[0.045, 1.1]}$ should be very approximately SM-like. It may thus be used as a control observable.
- The observable $\langle \hat{Q}_5 \rangle^{[1.1, 6]}$ emerges as a promising one

to discern the SM from Scenario 2, and the other four NP scenarios, depending on the experimental uncertainties.

► B_5 and B_{6s} in the first bin $[0.045, 1.1]$ are extremely sensitive to Scenario 2 and able to distinguish it from the Scenarios 1, 3 and 4 if small experimental uncertainties

can be achieved.

In the near future, precise measurements of these observables will thus be instrumental in establishing the NP patterns for LFUV discussed in this paper.

-
- [1] S. Descotes-Genon, T. Hurth, J. Matias and J. Virto, “Optimizing the basis of $B \rightarrow K^* \ell \ell$ observables in the full kinematic range,” JHEP **1305** (2013) 137 [arXiv:1303.5794 [hep-ph]].
- [2] LHCb Collaboration, “Measurement of Form-Factor-Independent Observables in the Decay $B^0 \rightarrow K^{*0} \mu^+ \mu^-$,” PRL **111** (2013) 191801 [arXiv:1308.1707 [hep-ex]].
- [3] S. Descotes-Genon, J. Matias and J. Virto, “Understanding the $B \rightarrow K^* \mu^+ \mu^-$ Anomaly,” Phys. Rev. D **88** (2013) 074002 [arXiv:1307.5683 [hep-ph]].
- [4] S. Descotes-Genon, J. Matias, M. Ramon and J. Virto, “Implications from clean observables for the binned analysis of $B \rightarrow K^* \mu^+ \mu^-$ at large recoil,” JHEP **1301** (2013) 048, [arXiv:1207.2753 [hep-ph]].
- [5] R. Aaij et al. [LHCb Collaboration], “Angular analysis of the $B^0 \rightarrow K^{*0} \mu^+ \mu^-$ decay using 3 fb^{-1} of integrated luminosity,” JHEP **1602** (2016) 104 [arXiv:1512.04442 [hep-ex]].
- [6] LHCb Collaboration, “Differential branching fraction and angular analysis of the decay $B_s^0 \rightarrow \phi \mu^+ \mu^-$,” JHEP **1307** (2013) 084 [arXiv:1305.2168 [hep-ex]].
- [7] LHCb Collaboration, “Angular analysis and differential branching fraction of the decay $B_s^0 \rightarrow \phi \mu^+ \mu^-$,” arXiv:1506.08777 [hep-ex].
- [8] A. Abdesselam et al. [Belle Collaboration], “Angular analysis of $B^0 \rightarrow K^*(892)^0 \ell^+ \ell^-$,” arXiv:1604.04042 [hep-ex].
- [9] S. Wehle et al. [Belle Collaboration], “Lepton-Flavor-Dependent Angular Analysis of $B \rightarrow K^* \ell^+ \ell^-$,” Phys. Rev. Lett. **118** (2017) no.11, 111801 [arXiv:1612.05014 [hep-ex]].
- [10] LHCb Collaboration, “Test of lepton universality using $B^+ \rightarrow K^+ \ell^+ \ell^-$ decays,” Phys. Rev. Lett. **113** (2014) 151601 [arXiv:1406.6482 [hep-ex]].
- [11] B. Capdevila, S. Descotes-Genon, J. Matias and J. Virto, “Assessing lepton-flavour non-universality from $B \rightarrow K^* \ell \ell$ angular analyses,” JHEP **1610** (2016) 075 [arXiv:1605.03156 [hep-ph]].
- [12] S. Descotes-Genon, L. Hofer, J. Matias and J. Virto, “Global analysis of $b \rightarrow s \ell \ell$ anomalies,” JHEP **1606** (2016) 092 [arXiv:1510.04239 [hep-ph]].
- [13] R. Aaij et al. [LHCb Collaboration], “Differential branching fractions and isospin asymmetries of $B \rightarrow K^{(*)} \mu^+ \mu^-$ decays,” JHEP **1406** (2014) 133 [arXiv:1403.8044 [hep-ex]].
- [14] R. Aaij et al. [LHCb Collaboration], “Measurements of the S-wave fraction in $B^0 \rightarrow K^+ \pi^- \mu^+ \mu^-$ decays and the $B^0 \rightarrow K^*(892)^0 \mu^+ \mu^-$ differential branching fraction,” JHEP **1611**, 047 (2016) [arXiv:1606.04731 [hep-ex]].
- [15] W. Altmannshofer and D. M. Straub, “New physics in $b \rightarrow s$ transitions after LHC run 1,” Eur. Phys. J. C **75** (2015) 8, 382 [arXiv:1411.3161 [hep-ph]].
- [16] W. Altmannshofer and D. M. Straub, “Implications of $b \rightarrow s$ measurements,” arXiv:1503.06199 [hep-ph].
- [17] T. Hurth, F. Mahmoudi and S. Neshatpour, “On the anomalies in the latest LHCb data,” Nucl. Phys. B **909** (2016) 737 [arXiv:1603.00865 [hep-ph]].
- [18] S. Jäger and J. Martin Camalich, “On $B \rightarrow V \ell \ell$ at small dilepton invariant mass, power corrections, and new physics,” JHEP **1305** (2013) 043 [arXiv:1212.2263 [hep-ph]].
- [19] S. Jäger and J. Martin Camalich, “Reassessing the discovery potential of the $B \rightarrow K^* \ell^+ \ell^-$ decays in the large-recoil region: SM challenges and BSM opportunities,” arXiv:1412.3183 [hep-ph].
- [20] M. Ciuchini, M. Fedele, E. Franco, S. Mishima, A. Paul, L. Silvestrini and M. Valli, “ $B \rightarrow K^* \ell^+ \ell^-$ decays at large recoil in the Standard Model: a theoretical reappraisal,” JHEP **1606** (2016) 116 [arXiv:1512.07157 [hep-ph]].
- [21] M. Ciuchini, M. Fedele, E. Franco, S. Mishima, A. Paul, L. Silvestrini and M. Valli, “ $B \rightarrow K^* \ell^+ \ell^-$ in the Standard Model: Elaborations and Interpretations,” arXiv:1611.04338 [hep-ph].
- [22] S. Descotes-Genon, L. Hofer, J. Matias and J. Virto, “On the impact of power corrections in the prediction of $B \rightarrow K^* \mu^+ \mu^-$ observables,” JHEP **1412** (2014) 125 [arXiv:1407.8526 [hep-ph]].
- [23] B. Capdevila, S. Descotes-Genon, L. Hofer and J. Matias, “Hadronic uncertainties in $B \rightarrow K^* \mu^+ \mu^-$: a state-of-the-art analysis,” JHEP **1704** (2017) 016 [arXiv:1701.08672 [hep-ph]].
- [24] V. G. Chobanova, T. Hurth, F. Mahmoudi, D. Martinez Santos and S. Neshatpour, “Large hadronic power corrections or new physics in the rare decay $B \rightarrow K^* \ell \ell$,” arXiv:1702.02234 [hep-ph].
- [25] R. Aaij et al. [LHCb Collaboration], “Measurement of the phase difference between short- and long-distance amplitudes in the $B^+ \rightarrow K^+ \mu^+ \mu^-$ decay,” Eur. Phys. J. C **77** (2017) 161 [arXiv:1612.06764 [hep-ex]].
- [26] The ATLAS collaboration [ATLAS Collaboration], “Angular analysis of $B_d^0 \rightarrow K^* \mu^+ \mu^-$ decays in pp collisions at $\sqrt{s} = 8 \text{ TeV}$ with the ATLAS detector,” ATLAS-CONF-2017-023.
- [27] CMS Collaboration [CMS Collaboration], “Measurement of the P_1 and P'_5 angular parameters of the decay $B^0 \rightarrow K^{*0} \mu^+ \mu^-$ in proton-proton collisions at $\sqrt{s} = 8 \text{ TeV}$,” CMS-PAS-BPH-15-008.
- [28] W. Altmannshofer, C. Niehoff, P. Stangl and D. M. Straub, “Status of the $B \rightarrow K^* \mu^+ \mu^-$ anomaly after Moriond 2017,” arXiv:1703.09189 [hep-ph].
- [29] S. Bifani (on behalf of the LHCb collaboration), “Search for new physics with $b \rightarrow s \ell \ell$ decays at LHCb,” seminar presented at CERN on 18 Apr 2017.
- [30] G. Hiller and M. Schmaltz, “Diagnosing lepton-nonuniversality in $b \rightarrow s \ell \ell$,” JHEP **1502** (2015) 055 [arXiv:1411.4773 [hep-ph]].
- [31] G. Hiller and M. Schmaltz, “ R_K and future $b \rightarrow s \ell \ell$

- physics beyond the standard model opportunities,” Phys. Rev. D **90** (2014) 054014 [arXiv:1408.1627 [hep-ph]].
- [32] Y. Amhis *et al.*, “Averages of b -hadron, c -hadron, and τ -lepton properties as of summer 2016,” arXiv:1612.07233 [hep-ex].
- [33] R. Aaij *et al.* [LHCb Collaboration], “Differential branching fraction and angular analysis of the decay $B^0 \rightarrow K^{*0} \mu^+ \mu^-$,” JHEP **1308**, 131 (2013) [arXiv:1304.6325 [hep-ex]].
- [34] S. Wehle, private communication.
- [35] V. Khachatryan *et al.* [CMS Collaboration], “Angular analysis of the decay $B^0 \rightarrow K^{*0} \mu^+ \mu^-$ from pp collisions at $\sqrt{s} = 8$ TeV,” Phys. Lett. B **753** (2016) 424 [arXiv:1507.08126 [hep-ex]].
- [36] S. Chatrchyan *et al.* [CMS Collaboration], “Angular analysis and branching fraction measurement of the decay $B^0 \rightarrow K^{*0} \mu^+ \mu^-$,” Phys. Lett. B **727** (2013) 77 [arXiv:1308.3409 [hep-ex]].
- [37] M. Misiak *et al.*, “Updated NNLO QCD predictions for the weak radiative B -meson decays,” Phys. Rev. Lett. **114** (2015) 22, 221801 [arXiv:1503.01789 [hep-ph]]. See also: T. Huber, M. Poradziński and J. Virto, “Four-body contributions to $\bar{B} \rightarrow X_s \gamma$ at NLO,” JHEP **1501**, 115 (2015) [arXiv:1411.7677 [hep-ph]]. M. Czakon, *et al.*, “The $(Q_7, Q_{1,2})$ contribution to $\bar{B} \rightarrow X_s \gamma$ at $\mathcal{O}(\alpha_s^2)$,” JHEP **1504**, 168 (2015) [arXiv:1503.01791 [hep-ph]].
- [38] T. Huber, T. Hurth and E. Lunghi, “Inclusive $\bar{B} \rightarrow X_s \ell^+ \ell^-$: complete angular analysis and a thorough study of collinear photons,” JHEP **1506**, 176 (2015) [arXiv:1503.04849 [hep-ph]].
- [39] C. Bobeth, M. Gorbahn, T. Hermann, M. Misiak, E. Stamou and M. Steinhauser, “ $B_{s,d} \rightarrow l^+ l^-$ in the Standard Model with Reduced Theoretical Uncertainty,” Phys. Rev. Lett. **112**, 101801 (2014) [arXiv:1311.0903 [hep-ph]].
- [40] A. Khodjamirian, T. Mannel, A. A. Pivovarov and Y.-M. Wang, “Charm-loop effect in $B \rightarrow K^{(*)} \ell^+ \ell^-$ and $B \rightarrow K^* \gamma$,” JHEP **1009**, 089 (2010) [arXiv:1006.4945 [hep-ph]].
- [41] A. Bharucha, D. M. Straub and R. Zwicky, “ $B \rightarrow V \ell^+ \ell^-$ in the Standard Model from light-cone sum rules,” JHEP **1608**, 098 (2016) [arXiv:1503.05534 [hep-ph]].
- [42] R. Gauld, F. Goertz and U. Haisch, “On minimal Z' explanations of the $B \rightarrow K^* \mu^+ \mu^-$ anomaly,” Phys. Rev. D **89** (2014) 015005 [arXiv:1308.1959 [hep-ph]].
- [43] A. J. Buras, F. De Fazio and J. Girrbach, “331 models facing new $b \rightarrow s \mu^+ \mu^-$ data,” JHEP **1402** (2014) 112 [arXiv:1311.6729 [hep-ph]].
- [44] S. Jäger, K. Leslie, M. Kirk and A. Lenz, “Charming new physics in rare B -decays and mixing?,” arXiv:1701.09183 [hep-ph].
- [45] P. Cox, A. Kusenko, O. Sumensari and T. T. Yanagida, “SU(5) Unification with TeV-scale Leptoquarks,” JHEP **1703** (2017) 035 [arXiv:1612.03923 [hep-ph]].
- [46] W. Altmannshofer, S. Gori, M. Pospelov and I. Yavin, “Quark flavour transitions in $L_\mu - L_\tau$ models,” Phys. Rev. D **89** (2014) 095033 [arXiv:1403.1269 [hep-ph]].
- [47] A. Crivellin, G. D’Ambrosio and J. Heeck, “Addressing the LHC flavour anomalies with horizontal gauge symmetries,” Phys. Rev. D **91** (2015) no.7, 075006 [arXiv:1503.03477 [hep-ph]].
- [48] A. Crivellin, J. Fuentes-Martin, A. Greljo and G. Isidori, “Lepton Flavor Non-Universality in B decays from Dynamical Yukawas,” Phys. Lett. B **766** (2017) 77 [arXiv:1611.02703 [hep-ph]].
- [49] A. Crivellin, G. D’Ambrosio and J. Heeck, “Explaining $h \rightarrow \mu^\pm \tau^\mp$, $B \rightarrow K^* \mu^+ \mu^-$ and $B \rightarrow K \mu^+ \mu^- / B \rightarrow K e^+ e^-$ in a two-Higgs-doublet model with gauged $L_\mu - L_\tau$,” Phys. Rev. Lett. **114** (2015) 151801 [arXiv:1501.00993 [hep-ph]].
- [50] D. Becirevic, S. Fajfer, N. Kosnik and O. Sumensari, “Leptoquark model to explain the B -physics anomalies, R_K and R_D ,” Phys. Rev. D **94** (2016) no.11, 115021 [arXiv:1608.08501 [hep-ph]].
- [51] D. Bhatia, S. Chakraborty and A. Dighe, “Neutrino mixing and R_K anomaly in $U(1)_X$ models: a bottom-up approach,” JHEP **1703** (2017) 117 [arXiv:1701.05825 [hep-ph]].
- [52] T. Araki, J. Heeck and J. Kubo, “Vanishing Minors in the Neutrino Mass Matrix from Abelian Gauge Symmetries,” JHEP **1207** (2012) 083 [arXiv:1203.4951 [hep-ph]].
- [53] G. Bélanger, C. Delaunay and S. Westhoff, “A Dark Matter Relic From Muon Anomalies,” Phys. Rev. D **92** (2015) 055021 [arXiv:1507.06660 [hep-ph]].
- [54] S. M. Boucenna, A. Celis, J. Fuentes-Martin, A. Vicente and J. Virto, “Non-abelian gauge extensions for B -decay anomalies,” Phys. Lett. B **760**, 214 (2016) [arXiv:1604.03088 [hep-ph]]. S. M. Boucenna, A. Celis, J. Fuentes-Martin, A. Vicente and J. Virto, “Phenomenology of an $SU(2) \times SU(2) \times U(1)$ model with lepton-flavour non-universality,” JHEP **1612** (2016) 059 [arXiv:1608.01349 [hep-ph]].
- [55] B. Gripaios, M. Nardecchia and S. A. Renner, “Composite leptoquarks and anomalies in B -meson decays,” JHEP **1505** (2015) 006 [arXiv:1412.1791 [hep-ph]].
- [56] S. Fajfer and N. Konik, “Vector leptoquark resolution of R_K and $R_{D^{(*)}}$ puzzles,” Phys. Lett. B **755** (2016) 270 [arXiv:1511.06024 [hep-ph]].
- [57] I. de Medeiros Varzielas and G. Hiller, “Clues for flavour from rare lepton and quark decays,” JHEP **1506** (2015) 072 [arXiv:1503.01084 [hep-ph]].
- [58] R. Alonso, B. Grinstein and J. Martin Camalich, “Lepton universality violation and lepton flavour conservation in B -meson decays,” JHEP **1510** (2015) 184 [arXiv:1505.05164 [hep-ph]].
- [59] L. Calibbi, A. Crivellin and T. Ota, “Effective Field Theory Approach to $b \rightarrow s \ell \ell$, $B \rightarrow K^{(*)} \nu \bar{\nu}$ and $B \rightarrow D^{(*)} \tau \nu$ with Third Generation Couplings,” Phys. Rev. Lett. **115** (2015) 181801 [arXiv:1506.02661 [hep-ph]].
- [60] R. Barbieri, G. Isidori, A. Pattori and F. Senia, “Anomalies in B -decays and $U(2)$ flavour symmetry,” Eur. Phys. J. C **76** (2016) no.2, 67 [arXiv:1512.01560 [hep-ph]].
- [61] B. Gripaios, M. Nardecchia and S. A. Renner, “Linear flavour violation and anomalies in B physics,” JHEP **1606** (2016) 083 [arXiv:1509.05020 [hep-ph]].
- [62] P. Arnan, L. Hofer, F. Mescia and A. Crivellin, “Loop effects of heavy new scalars and fermions in $b \rightarrow s \mu^+ \mu^-$,” arXiv:1608.07832 [hep-ph].
- [63] F. Mahmoudi, S. Neshatpour and J. Virto, “ $B \rightarrow K^* \mu^+ \mu^-$ optimised observables in the MSSM,” Eur. Phys. J. C **74**, 6, 2927 (2014) [arXiv:1401.2145 [hep-ph]].
- [64] S. Descotes-Genon and J. Virto, “Time dependence in $B \rightarrow V \ell \ell$ decays,” JHEP **1504** (2015) 045 Erratum: [JHEP **1507** (2015) 049] [arXiv:1502.05509 [hep-ph]].
- [65] R. Aaij *et al.* [LHCb Collaboration], “Measurement of the $B_s^0 \rightarrow \mu^+ \mu^-$ branching fraction and effective lifetime

- and search for $B^0 \rightarrow \mu^+ \mu^-$ decays,” arXiv:1703.05747 [hep-ex].
- [66] K. De Bruyn, R. Fleischer, R. Kneijens, P. Koppenburg, M. Merk, A. Pellegrino and N. Tuning, “Probing New Physics via the $B_s^0 \rightarrow \mu^+ \mu^-$ Effective Lifetime,” Phys. Rev. Lett. **109**, 041801 (2012) [arXiv:1204.1737 [hep-ph]].
- [67] A. Crivellin, G. D’Ambrosio, M. Hoferichter and L. C. Tunstall, “Violation of lepton flavor and lepton flavor universality in rare kaon decays,” Phys. Rev. D **93** (2016) no.7, 074038 [arXiv:1601.00970 [hep-ph]].
- [68] R. Alonso, B. Grinstein and J. Martin Camalich, “The lifetime of the B_c^- meson and the anomalies in $B \rightarrow D^{(*)} \tau \nu$,” Phys. Rev. Lett. **118** (2017) no.8, 081802 [arXiv:1611.06676 [hep-ph]].
- [69] M. Freytsis, Z. Ligeti and J. T. Ruderman, “Flavor models for $\bar{B} \rightarrow D^{(*)} \tau \bar{\nu}$,” Phys. Rev. D **92** (2015) no.5, 054018 [arXiv:1506.08896 [hep-ph]].
- [70] A. Celis, M. Jung, X. Q. Li and A. Pich, “Scalar contributions to $b \rightarrow c(u) \tau \nu$ transitions,” arXiv:1612.07757 [hep-ph].
- [71] M. A. Ivanov, J. G. Krner and C. T. Tran, “Probing new physics in $\bar{B}^0 \rightarrow D^{(*)} \tau^- \bar{\nu}_\tau$ using the longitudinal, transverse, and normal polarization components of the tau lepton,” Phys. Rev. D **95** (2017) no.3, 036021 [arXiv:1701.02937 [hep-ph]].
- [72] D. A. Faroughy, A. Greljo and J. F. Kamenik, “Confronting lepton flavor universality violation in B decays with high- p_T tau lepton searches at LHC,” Phys. Lett. B **764** (2017) 126 [arXiv:1609.07138 [hep-ph]].
- [73] F. Feruglio, P. Paradisi and A. Pattori, “Revisiting Lepton Flavor Universality in B Decays,” Phys. Rev. Lett. **118** (2017) no.1, 011801 [arXiv:1606.00524 [hep-ph]].
- [74] B. Grzadkowski, M. Iskrzynski, M. Misiak and J. Rosiek, “Dimension-Six Terms in the Standard Model Lagrangian,” JHEP **1010** (2010) 085 [arXiv:1008.4884 [hep-ph]].
- [75] A. Crivellin, D. Müller and T. Ota, “Simultaneous Explanation of $R_{D^{(*)}}$ and $b \rightarrow s \mu^+ \mu^-$: The Last Scalar Leptoquarks Standing,” arXiv:1703.09226 [hep-ph].